

Contents lists available at SciVerse ScienceDirect

## **Optical Materials**

journal homepage: www.elsevier.com/locate/optmat



# Near- and mid-infrared emissions from $Dy^{3+}$ and $Nd^{3+}$ -doped $Ga_2S_3-GeS_2-Sb_2S_3$ glass



M. Ichikawa, Y. Ishikawa, T. Wakasugi, K. Kadono\*

Graduate School of Chemistry and Materials Technology, Kyoto Institute of Technology, Matsugasaki, Sakyo-ku, Kyoto 606-8585, Japan

#### ARTICLE INFO

Article history:
Available online 8 February 2013

Keywords: Sulfide glass Rare-earth Infrared emission Energy transfer Low-phonon energy Judd-Ofelt analysis

#### ABSTRACT

Dy³+- and Nd³+-doped stoichiometric  $20GaS_{3/2}$ : $50GeS_2$ : $30SbS_{3/2}$  glasses were prepared. Judd-Ofelt analyses were performed to estimate radiative transition parameters for the excited levels. Near- and midinfrared emission spectra were observed and their emission bands were carefully assigned on the basis of the transition parameters and the comparison of the spectra obtained by the different excited levels. The 4.4-µm emission band from Dy³+ due to the transition,  ${}^6H_{11/2} \rightarrow {}^6H_{13/2}$ , had a branching ratio more than 10% and a quantum efficiency was 63% for the glass doped with 0.3 mol% of DyS<sub>3/2</sub>. The radiative transition rate of the initial level for this transition,  ${}^6H_{11/2}$ , is larger than that of the final level,  ${}^6H_{13/2}$ . However, the latter was more rapidly quenched at higher Dy concentration, which means that the problem of the self-termination for the four-level system could be avoided at an adequate concentration range.

© 2013 Elsevier B.V. All rights reserved.

#### 1. Introduction

Because of the low phonon energy and the high refractive index, chalcogenide glasses have received much attention as host materials of rare-earth ions in order to obtain efficient emission in the near- and mid-infrared regions [1,2]. Among the various kinds of chalcogenide glass systems, the Ga-Ge-Sb-S or the stoichiometric Ga<sub>2</sub>S<sub>3</sub>-GeS<sub>2</sub>-Sb<sub>2</sub>S<sub>3</sub> system is noteworthy because it has other additive advantages as host materials; the glasses based on this system have high solubility of rare-earth ions and relatively wide optical window at the short wavelength side. The latter is attractive because of the possibility to use low-cost laser diodes with wavelength shorter than  $1 \, \mu m$  for the excitation of rare-earth ions. In fact, high efficient emissions in the mid-infrared region have been reported for Er3+-doped or Ho3+-doped Ga-Ge-Sb-S or Ga2S3-GeS<sub>2</sub>–Sb<sub>2</sub>S<sub>3</sub> glasses [3–7]. Since Nd<sup>3+</sup> and Dy<sup>3+</sup> have been regarded as an alternative candidate for mid-infrared emission [1,2,8-14], in this article, we report emission characteristics of these ions embedded in the Ga<sub>2</sub>S<sub>3</sub>-GeS<sub>2</sub>-Sb<sub>2</sub>S<sub>3</sub> glasses.

When we use mid-infrared emissions from rare-earth ions with the excitation at a wavelength shorter than 1  $\mu$ m, in most of the cases, the laser scheme is a four-level system. Then, we are frequently faced with the problem in which the lifetime of the final level is longer than that of the initial level resulting in the self-termination of laser oscillation [15]. To resolve this problem, it is known that using the aid of energy transfer processes between

the rare-earth ions is very effective to quench the population of the final level. Then, particularly, we investigated the Dy concentration dependence on the emission behaviors for the Dy<sup>3+</sup>-doped glass.

#### 2. Experimental procedures

Glasses with composition  $20\text{GaS}_{3/2} \cdot 50\text{GeS}_2 \cdot 30\text{SbS}_{3/2} \cdot x\text{DyS}_{3/2}$  (x = 0.3, 1, and 3 mol% corresponding to the number density of Dy³+, 0.411, 1.36, and  $4.02 \times 10^{20}$  cm³, respectively) and  $20\text{GaS}_{3/2} \cdot 50\text{GeS}_2 \cdot 30\text{SbS}_{3/2} \cdot 3N\text{dS}_{3/2}$  (the number density of Nd³+,  $4.05 \times 10^{20}$  cm³) were prepared in sealed silica tubes from batch mixtures consisting of elements (Ga (7N), Ge (4N), Sb (5Nup), and S (6N)) and Dy (3N) metal or Nd<sub>2</sub>S<sub>3</sub> (3N). More detail description for the glass preparation is found elsewhere [5]. The glass transition temperature, density, and refractive index at 980 nm of the undoped host glass,  $20\text{GaS}_{3/2} \cdot 50\text{GeS}_2 \cdot 30\text{SbS}_{3/2}$ , were 321 °C, 3.26 g cm³, and 2.31, respectively.

Absorption spectra were measured using a spectrophotometer (UV-3100, Shimadzu) in the wavelength range from 400 to 2000 nm and FT-IR spectrometer (JIR-WINSPEC50, JEOL) in the range from 400 to 7000 cm $^{-1}$ . The emission spectra in the infrared regions were measured by exciting well-polished glasses using a Ti:sapphire laser. The emissions from the sides of the samples were detected by an InSb detector (EG&G) cooled at liq. N<sub>2</sub> temperature. The spectra were not corrected for the spectral response of the detector in the present experiments. The lifetimes of the excited levels were determined as 1/e holding times of the decay curves of the emission from the levels. The pulsed laser beam to measure

<sup>\*</sup> Corresponding author. Tel./fax: +81 75 724 7565. E-mail address: kadono@kit.ac.jp (K. Kadono).

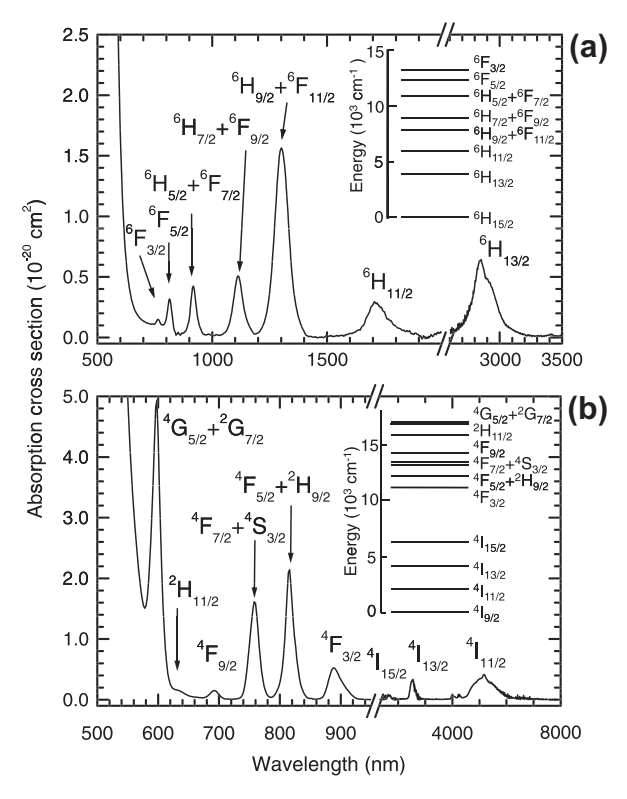


**Fig. 1.** Absorption spectra for (a)  $20GaS_{3/2} \cdot 50GeS_2 \cdot 30SbS_{3/2} \cdot 1DyS_{3/2}$  and (b)  $20GaS_{3/2} \cdot 50GeS_2 \cdot 30SbS_{3/2} \cdot 3NdS_{3/2}$  glasses. The ordinate is presented as the absorption cross section.

the decay curves was obtained by chopping the c.w. laser beam with a mechanical chopper.

#### 3. Results and discussion

#### 3.1. Absorption spectra and Judd-Ofelt analyses

Fig. 1 shows the absorption spectra presented with cross sections of  $20\text{GaS}_{3/2} \cdot 50\text{GeS}_2 \cdot 30\text{SbS}_{3/2} \cdot 10\text{yS}_{3/2}$  and  $20\text{GaS}_{3/2} \cdot 50\text{GeS}_2 \cdot 30\text{SbS}_{3/2} \cdot 30\text{MdS}_{3/2}$  glasses. Since the absorption edge at the short wavelength side of the host glass is around 600 nm, absorption bands to the  $^6\text{F}_{3/2}$  and to the  $^4\text{G}_{5/2}$ ,  $^2\text{G}_{7/2}$  were observed for the Dy³+ and Nd³+-doped glasses, respectively. Judd–Ofelt analyses were performed using these observed bands except for the lowest-excited levels, respectively, which have a large contribution from a magnetic dipole transition. The obtained omega parameters and transition characteristics for lower several excited levels are summarized in Tables 1 and 2. Lifetimes, nonradiative transition rates, and quantum efficiencies for the lowest three excited levels in Dy³+ are also presented.

#### 3.2. Near- and mid-infrared emission spectra

Near- and mid-infrared emission spectra are shown for Dydoped and Nd-doped glasses in Figs. 2 and 3, respectively. For the Dy-doped glass, the spectra in the near-infrared region were measured with the excitation at the  $^6F_{3/2}$  (765 nm),  $^6F_{5/2}$  (814 nm), and  $^6H_{5/2}+^6F_{7/2}$  (918 nm) levels. Since the emission spectra obtained with the excitation at  $^6F_{3/2}$  and  $^6F_{5/2}$  were the same, only the spectra with the excitation at the  $^6F_{5/2}$ , and  $^6H_{5/2}+^6F_{7/2}$  are shown. Four emission bands at 1150, 1320, 1550, and 1740 nm were observed in the near-infrared region for the Dy-doped glass with the excitation at  $^6F_{3/2}$  and  $^6F_{5/2}$ . However,

the 1150-nm and 1550-nm bands disappeared with the excitation at  ${}^{6}H_{5/2} + {}^{6}F_{7/2}$ . Then these bands were assigned to the transitions,  $^6F_{5/2} \rightarrow ^6H_{13/2}$  and  $^6F_{5/2} \rightarrow ^6H_{11/2}$ , respectively. The 1320-nm band was assigned to  $^6H_{9/2} + ^6F_{11/2} \rightarrow ^6H_{15/2}$ . Both transitions,  $^{6}\text{H}_{11/2} \rightarrow ^{6}\text{H}_{15/2}$  and  $^{6}\text{H}_{7/2} + ^{6}\text{F}_{9/2} \rightarrow ^{6}\text{H}_{13/2}$ , were considered as an origin of the 1740-nm band. If the emission from the  $^6\mathrm{H}_{7/2}$  +  $^6F_{9/2} \rightarrow ^6H_{13/2}$  transition were included in the 1740-nm band, the emission from the  ${}^6{\rm H}_{7/2}$  +  ${}^6{\rm F}_{9/2}$   $\rightarrow$   ${}^6{\rm H}_{15/2}$  transition should be observed around 1100 nm because the branching ratio of the latter transition is larger than that of the former transition (see Table 1). However, the 1100-nm emission band was not observed. Then, the contribution from the  ${}^6\mathrm{H}_{7/2}$  +  ${}^6\mathrm{F}_{9/2}$   $\rightarrow$   ${}^6\mathrm{H}_{13/2}$  transition to the 1740nm band was supposed to be small. Therefore, the band was assigned to the  ${}^6H_{11/2} \rightarrow {}^6H_{15/2}$  transition. In the mid-infrared region, two bands assigned to the transition,  ${}^6H_{13/2} \rightarrow {}^6H_{15/2}$  and  $^6\text{H}_{11/2} \rightarrow ^6\text{H}_{13/2}$ , were observed around 2.98 µm and 4.38 µm, respectively. Among these assignments for the emission bands of the Dy-doped glass, the bands due to the transitions from the levels,  ${}^6\mathrm{H}_{5/2}$  +  ${}^6\mathrm{F}_{7/2}$  and  ${}^6\mathrm{H}_{7/2}$  +  ${}^6\mathrm{F}_{9/2}$ , were not observed. For the  $^6\mathrm{H}_{7/2}$  +  $^6\mathrm{F}_{9/2}$ , this is attributed to the large multiphonon relaxation rate because of the small energy gap to the next lower level,  $^6\mathrm{H}_{9/2}$  +  $^6\mathrm{F}_{11/2}$ . On the other hand, the energy gap between the  $^6\mathrm{H}_{5/2}$  +  $^6\mathrm{F}_{7/2}$  and the next lower level,  $^6\mathrm{H}_{7/2}$  +  $^6\mathrm{F}_{9/2}$ , is supposed to be similar to that between  ${}^6H_{9/2}$  +  ${}^6F_{11/2}$  and  ${}^6H_{11/2}$ , and even larger than that between  ${}^6F_{5/2}$  and  ${}^6H_{5/2}$  +  ${}^6F_{7/2}$ . Therefore, the main reason for the absence of the emission from the  ${}^6{\rm H}_{5/2}$  +  ${}^6{\rm F}_{7/2}$  is not the multiphonon relaxation but the small radiative transition rate from this level as shown in Table 1. Then, for the Dy-doped glass, the emissions which were observed were assigned only to the transitions from the levels,  ${}^{6}F_{5/2}$ ,  ${}^{6}H_{9/2} + {}^{6}F_{11/2}$ ,  ${}^{6}H_{11/2}$ , and  ${}^{6}H_{13/2}$ .

The near-infrared emissions at 900, 970, 1080, 1195, and 1370 nm for the Nd-doped glass were assigned as shown in Fig. 3a. In the mid-infrared region, two bands were observed. The band observed around 2.54  $\mu$ m was assigned to the transition  ${}^4I_{13/2} \rightarrow {}^4I_{9/2}$ . On the other hand, at least three transitions,  ${}^4I_{11/2} \rightarrow {}^4I_{9/2}$ ,  ${}^4I_{13/2} \rightarrow {}^4I_{11/2}$ , and  ${}^4I_{15/2} \rightarrow {}^4I_{13/2}$  are considered to be an origin for the broad band around 5  $\mu$ m; these transitions have comparable radiative transition rates as shown in Table 2. The rate of the multiphonon relaxation should be small because of the large energy gap between the  ${}^4F_{3/2}$  and  ${}^4I_{15/2}$ , and radiative transition rates from  ${}^4F_{3/2}$  to  ${}^4I_{11/2}$  is much larger than those of the transitions to  ${}^4I_{13/2}$  and  ${}^4I_{15/2}$  as shown in Table 2. Therefore, since the population at the  ${}^4I_{11/2}$  is expected to be larger than those of  ${}^4I_{13/2}$  and  ${}^4I_{15/2}$ , the main contribution to the 5- $\mu$ m band was predicted to be the transition,  ${}^4I_{11/2} \rightarrow {}^4I_{9/2}$ .

#### 3.3. Energy transfer in Dy-doped glass

Fig. 4 shows the near-infrared emission spectra of glasses doped with different amount of Dy measured with the excitation of the <sup>6</sup>F<sub>5/2</sub> level. The emission intensities of these spectra are normalized at that of the 1320-nm emission. With increasing the Dy concentration, the intensities of the 1150-nm and 1550-nm emission bands relatively increased against that of the 1320-nm band while that of the 1740-nm band decreased. When the  ${}^{6}H_{5/2} + {}^{6}F_{7/2}$  levels were excited, the relative intensity of the 1740-nm band against that of the 1320-nm band deceased as well as in the case of the <sup>6</sup>F<sub>5/2</sub> level excitation although the 1150-nm and 1550-nm bands were not observed. In the inset of Fig. 5, the decays of the 2.9- $\mu$ m emission from the  $^6H_{13/2}$  level are shown. The emission more rapidly decayed in the glass doped with more amount of Dy. Fig. 5 shows the Dy concentration dependences of the emission lifetimes at 2.9  $\mu$ m, 1740 nm, and 1320 nm from  ${}^6H_{13/2}$ ,  ${}^6H_{11/2}$ , and  ${}^{6}H_{9/2} + {}^{6}F_{11/2}$ , respectively. All these lifetimes were shortened with the Dy concentration because of various energy transfer processes. Heo et al. argued that the cross relaxation ( ${}^{6}H_{13/2}$ ,

### Download English Version:

# https://daneshyari.com/en/article/1494474

Download Persian Version:

https://daneshyari.com/article/1494474

<u>Daneshyari.com</u>